DISCRETE VORTEX SIMULATION OF FLOW OVER A BLUFF BODY

K.Hourigan*

Introduction

A feature very prominent in high Reynolds-number flows around bluff bodies is that of separation of turbulent shear layers, which may or may not reattach. From a numerical modelling point of view, it can be convenient to view these flows as being characterized by regions of concentrated vorticity embedded in irrotational fluid. The local fluid velocity, which is determined kinematically from the vorticity field, then determines the inviscid motion of the vorticity. This type of flow is simulated by the discrete-vortex model by replacing the regions of vorticity concentration with elemental vortices, whose motions are followed in a Lagrangian reference frame. Thus, provided the location and rates of vorticity production can be specified fairly readily, the costly exercise of solving the full Navier-Stokes equations can be avoided.

Although the discrete-vortex model was first devised over fifty years ago [1], most of its development and application have taken place in more recent years. It has been successfully applied to the simulation of the roll-up of free vortex sheets [2]. However, some ad hoc assumptions in respect of vorticity loss have had to be introduced in problems where reattachment of the shear layers takes place. That is, it appears that surface viscous effects cannot be ignored. Successfully incorporating these effects into the discrete vortex model remains a challenging problem.

In this paper, the various steps involved in the construction of a discrete-vortex model are discussed. The simple geometry of the example problem provided, viz. flow over a forward-facing step, allows a fairly straightforward analysis of the basic ingredients of the model. It should be noted however, that the discrete-vortex model is, in principle, capable of simulating flows around some of the more complex geometries that are encountered in wind engineering and industrial aerodynamics.

Description of the Model

The geometry of the flow situation of interest is shown in Figure 1(a). It is important in the first instance to be able to identify points of significant vorticity production. The top corner of the step is obviously one such point where separation occurs. The separated shear layer is then represented by a system of line vortices. In order to satisfy the condition of zero flow normal to the solid boundary, a transformed complex plane is considered in which image vortices are appropriately positioned. In the present problem, the region in the physical z plane representing the flow region was conformally mapped onto the upper half of another complex plane, the λ plane.

The complex velocity potential Φ then consists of two components due to the irrotational flow Φ_i and the flow induced by the vortices Φ_v

$$\Phi = \Phi_i + \Phi_v = V_o(H/\pi)\lambda + \sum_{j=1}^{n} \frac{iG_j}{2\pi} \{\log(\lambda-\lambda_j) - \log(\lambda - \lambda^*_j)\} ,$$

where V_o is the velocity at upstream infinity, H is the step height, λ_j is the location of the j^{th} vortex, λ^*_j denotes its complex conjugate, and G_j represents its circulation. The velocity field u-iv in the physical plane is given by $d\Phi/dz$ except at the vortex points where it is given by

---

* CSIRO Division of Energy Technology, Melbourne, Australia

$$\lim_{z \to z_k} \frac{d}{dz} \left(\Phi - \frac{iG_k}{2\pi} \log (z - z_k) \right).$$

A time-stepping integration scheme is then introduced to follow the evolution of the vortices according to these non-linear DE's.

A determination is now required of the strength G of each elemental vortex and its nascent position. The rate of creation of vorticity at a separation point is determined by the kinematic condition $dG/dt = -\frac{1}{2}(u_+^2 - u_-^2)$, where u_+ and u_- are the higher and lower speeds on either side of the separating shear layer. Given an integration scheme timestep, the strength of each nascent vortex can then be allotted. In order to determine the position of a nascent vortex, the Kutta condition is invoked. This condition requires that the velocity $d\Phi/d\lambda$ at the point in the transformed plane corresponding to the step corner is zero.

The initial conditions are now completely specified. It is found however in the present problem that restricting vorticity generation to the leading edge does not produce a satisfactory simulation. In order to match experimental results, it has been found necessary by users of the discrete-vortex model to incorporate a temporal reduction of circulation of the elemental vortices (e.g. [3]). Although this is inconsistent with vorticity conservation required by inviscid-flow theory, it has been suggested that the circulation reduction allows for viscous and three-dimensional effects that would occur in real flows [4]. However, here it is argued that generation of vorticity of opposite sign to that generated at the leading edge will take place along the step surface. From the momentum equation and the condition of no-slip, it can be shown that the flux of circulation is proportional to the pressure gradient along the surface. A separation bubble represents a region of sustained large pressure gradients and therefore a source of significant vorticity. The overall circulation is then reduced as a result of diffusion of this opposite signed vorticity.

Often of interest in practical applications, of course, are the pressure and velocity distributions, especially near the surfaces. The instantaneous velocity field can be found from the velocity potential as mentioned above. The instantaneous pressures p can be determined from the model by making use of the Bernoulli equation for the pressure coefficient C_p

$$C_p = \frac{p - p_o}{\frac{1}{2}\rho V_o^2} = 1 - \frac{2}{V_o^2} \operatorname{Re}\left(\frac{\partial \Phi}{\partial t}\right) - \frac{1}{V_o^2} \left|\frac{d\Phi}{dz}\right|^2,$$

where p_o is the pressure of the free stream and ρ is the density of the fluid.

Numerical Results and Discussion

In this section, some sample results of the model described above are included. Figure 1(a) shows a snapshot of the positions of the elemental vortices at a time when the mean flow had become statistically stationary. The roll-up of the shear layer into larger-scale vorticial structures can perhaps be seen more clearly in Figure 1(b), which shows the trajectories of the elemental vortices over a short time period. It can be seen that the shedding of vortices from the separation bubble does not take place periodically, in line with experimental results. The vortices traversing the surface are of varying size and the vortex spacing is irregular.

In Figure 1(c), the fluctuating surface pressures, at the same instant of time as above, are shown in addition to the time-mean surface pressure distribution. Comparing Figures 1(b) and 1(c), it can be seen that the fluctuating surface pressure is negative beneath the large-scale vortices and positive in the regions between these vortices.

In conclusion, the discrete-vortex model is found to be capable of simulating at least some of the gross characteristics of separated flow from a leading edge. A feature of the model is its ability to predict instantaneous velocities and pressures, the knowledge of which is important in areas such as structure design and heat transfer. Furthermore, prediction of the location of vorticity can enable determination of sound source regions and the development of acoustic resonances [5].

References

1. L.Rosenhead, 'The Formation of Vortices from a Surface of Discontinuity', Proc.R.Soc., Lond. 134, 170, 1931.

2. D.W.Moore, 'A Numerical Study of the Roll-up of a Finite Vortex Sheet', J.Fluid Mech., 63, 225, 1974.

3. T.Sarpkaya and R.L.Shoaf, 'Inviscid Model of Two-dimensional Vortex Shedding by a Circular Cylinder', A.I.A.A.J., 17, 1193, 1979.

4. M.Kiya, K.Sasaki and M.Arie, 'Discrete-vortex Simulation of a Turbulent Separation Bubble', 120, 219, 1982.

5. M.C.Welsh, A.N.Stokes and R.Parker, 'Flow-resonant Sound Interaction in a Duct Containing a Plate. Part I: Semi-circular Leading Edge', J.Sound and Vibration to be published (1984).

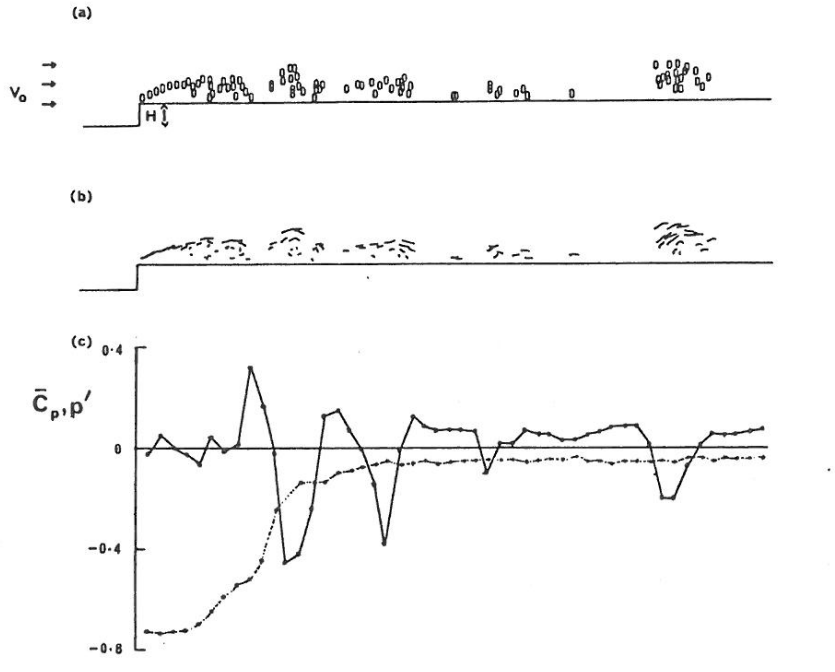

Figure 1: (a) snapshot of elemental vortex positions
(b) vortex trajectories
(c) mean surface-pressure coefficient $\bar{C}_p$ (broken line) and surface-pressure fluctuations p' (solid line).